Exploring the free energy landscape: Comparison of kinetic models for MgO-catalyzed ethanol conversion to 1,3-butadiene

Astrid Boje, William E. Taifan, Henrik Ström, Tomáš Bučko, Jonas Baltrusaitis, and Anders Hellman

7 April 2021

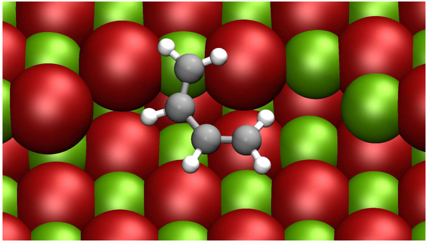

Ethanol-to-butadiene: process, impact and limitations

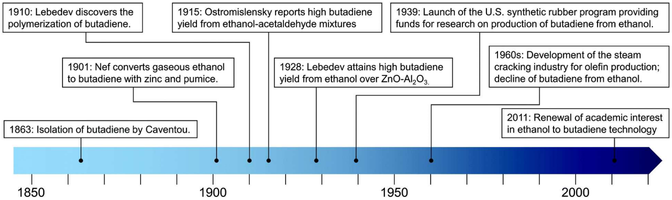

Timeline of developments

Pomalaza *et al.*, Catal. Sci. Technol., 2020, 10, 4860.

Ethanol-to-butadiene: process, impact and limitations

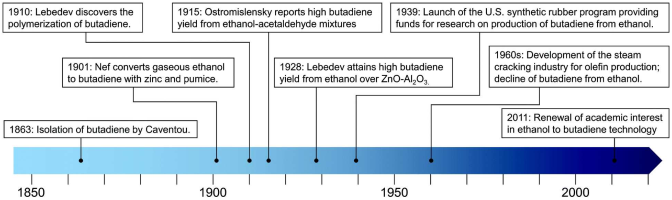

Timeline of developments

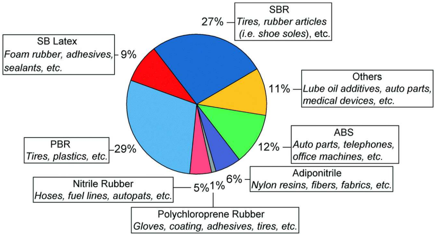

Product uses (2015)

Pomalaza *et al.*, Catal. Sci. Technol., 2020, 10, 4860.

Ethanol-to-butadiene: process, impact and limitations

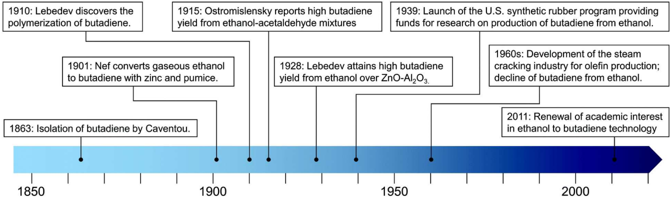

Timeline of developments

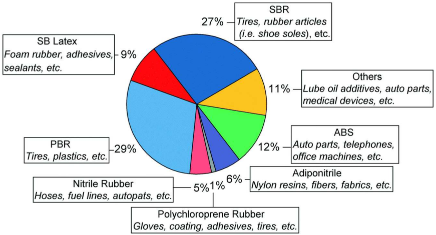

Product uses (2015)

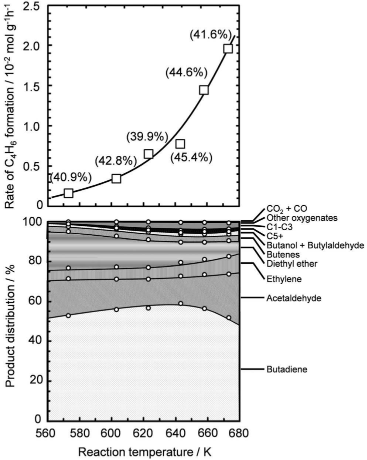

With temperature (talc/Zn)

Pomalaza *et al.*, Catal. Sci. Technol., 2020, 10, 4860.

Hayashi *et al.*, Phys. Chem. Chem. Phys., 2016, 18, 25191.

Ethanol-to-butadiene on an MgO (100) step edge

MgO slab with stepped kink

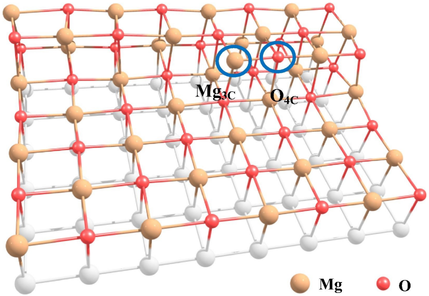

DFT calculations: PBE with PAW, 400 eV cutoff, 2×2×1 *k*-points.

Taifan *et al.*, J. Catal., 2017, 346, 78.

Ethanol-to-butadiene on an MgO (100) step edge

MgO slab with stepped kink

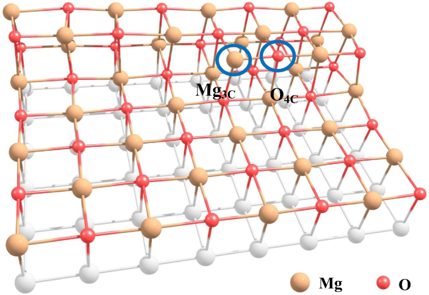

DFT calculations: PBE with PAW, 400 eV cutoff, 2×2×1 *k*-points.

Key reaction steps:

Taifan *et al.*, J. Catal., 2017, 346, 78.

Ethanol-to-butadiene on an MgO (100) step edge

MgO slab with stepped kink

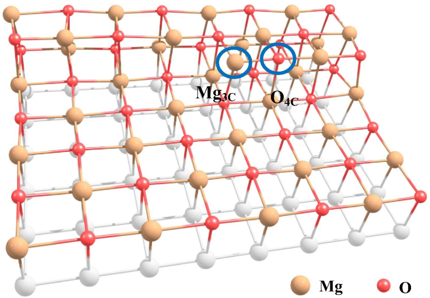

DFT calculations: PBE with PAW, 400 eV cutoff, 2×2×1 *k*-points.

Key reaction steps:

- Ethanol **dehydrogenation** to acetaldehyde

Taifan *et al.*, J. Catal., 2017, 346, 78.

Ethanol-to-butadiene on an MgO (100) step edge

MgO slab with stepped kink

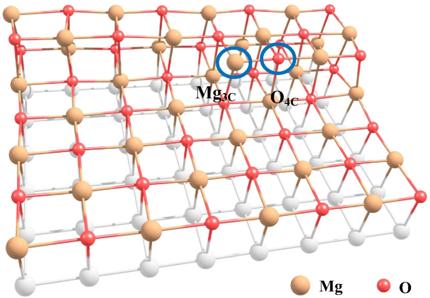

DFT calculations: PBE with PAW, 400 eV cutoff, 2×2×1 *k*-points.

Key reaction steps:

- Ethanol **dehydrogenation** to acetaldehyde
- Ethanol **dehydration** to ethylene

Taifan *et al.*, J. Catal., 2017, 346, 78.

Ethanol-to-butadiene on an MgO (100) step edge

MgO slab with stepped kink

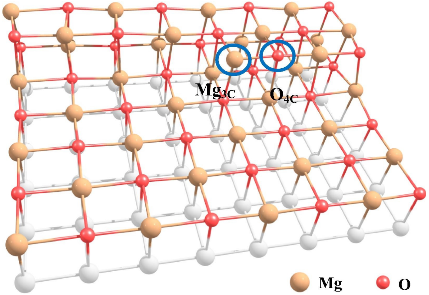

DFT calculations: PBE with PAW, 400 eV cutoff, 2×2×1 k-points.

Key reaction steps:

- Ethanol **dehydrogenation** to acetaldehyde
- Ethanol **dehydration** to ethylene
- C–C bond formation by **condensation**

Taifan *et al.*, J. Catal., 2017, 346, 78.

Ethanol-to-butadiene on an MgO (100) step edge

MgO slab with stepped kink

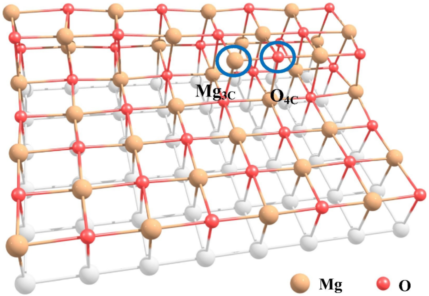

DFT calculations: PBE with PAW, 400 eV cutoff, 2×2×1 *k*-points.

Key reaction steps:

- Ethanol **dehydrogenation** to acetaldehyde
- Ethanol **dehydration** to ethylene
- C–C bond formation by **condensation**
- MPV **reduction** of acetaldol and crotonaldehyde

Taifan *et al.*, J. Catal., 2017, 346, 78.

Ethanol-to-butadiene on an MgO (100) step edge

MgO slab with stepped kink

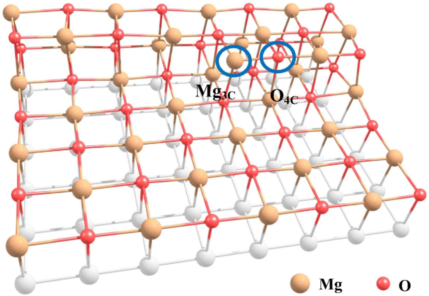

DFT calculations: PBE with PAW, 400 eV cutoff, 2×2×1 *k*-points.

Key reaction steps:

- Ethanol **dehydrogenation** to acetaldehyde
- Ethanol **dehydration** to ethylene
- C–C bond formation by **condensation**
- MPV **reduction** of acetaldol and crotonaldehyde

Multiple reaction pathways

Taifan *et al.*, J. Catal., 2017, 346, 78.

Several possible pathways convert ethanol to butadiene

Reactant

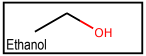

Product

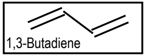

Several possible pathways convert ethanol to butadiene

p123

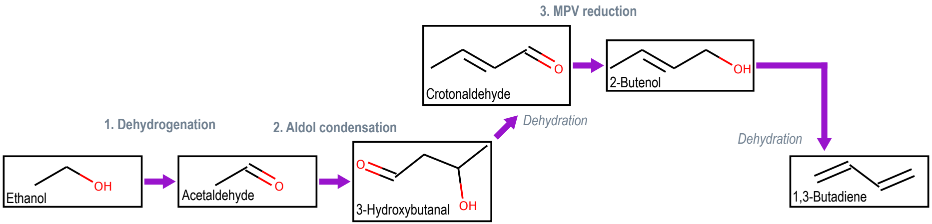

Several possible pathways convert ethanol to butadiene

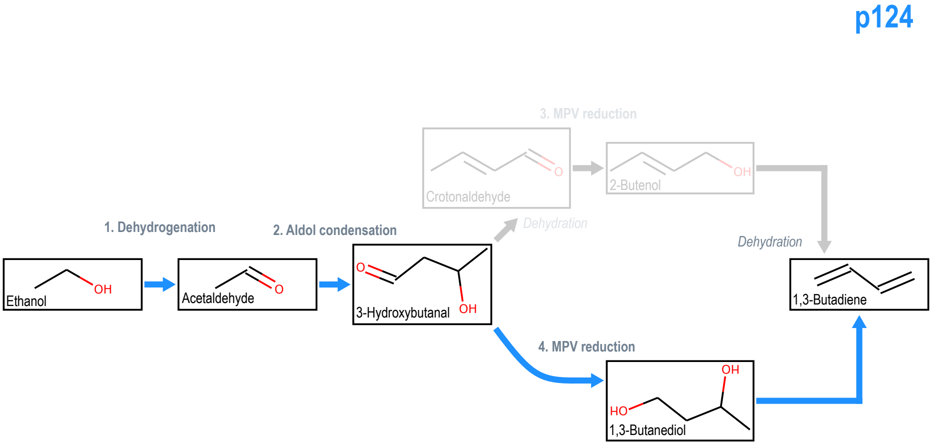

Several possible pathways convert ethanol to butadiene

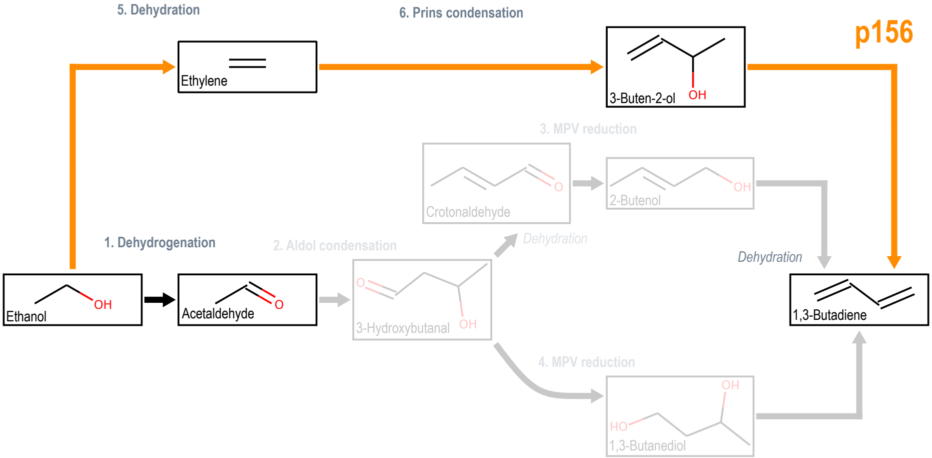

Several possible pathways convert ethanol to butadiene

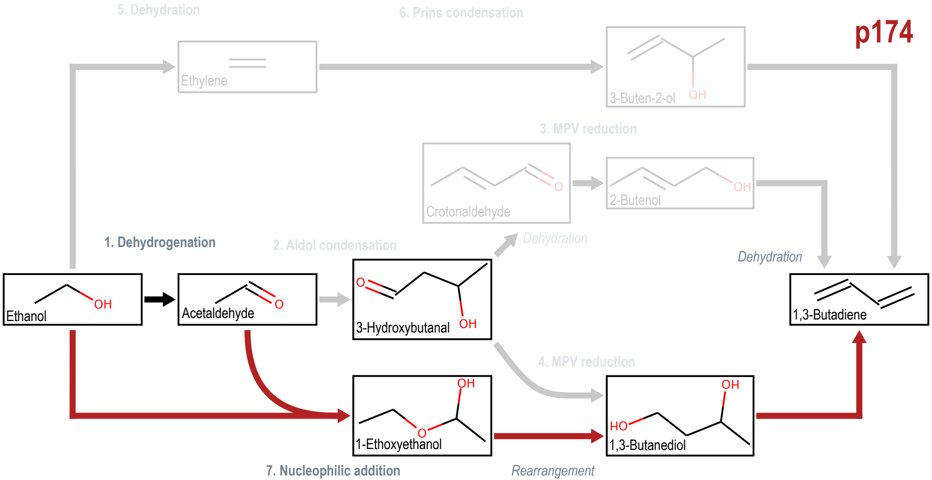

Several possible pathways convert ethanol to butadiene

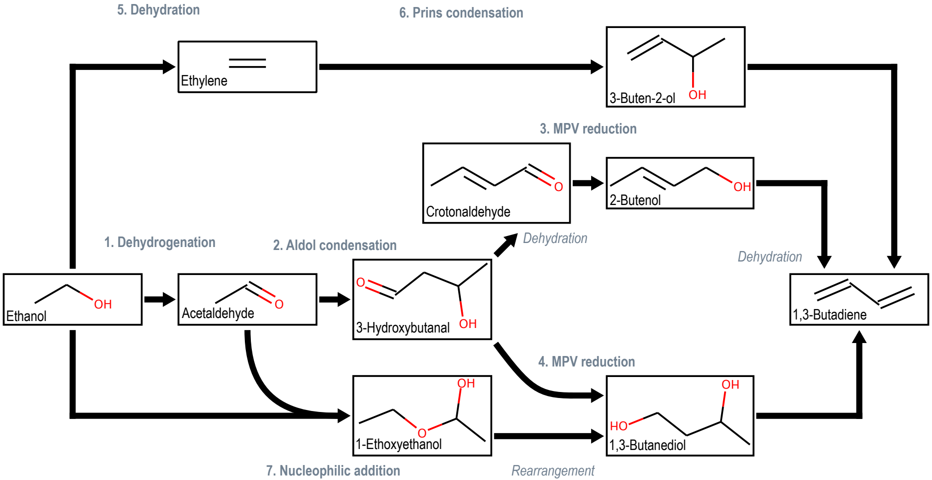

Two perspectives on first-principles based kinetic modelling

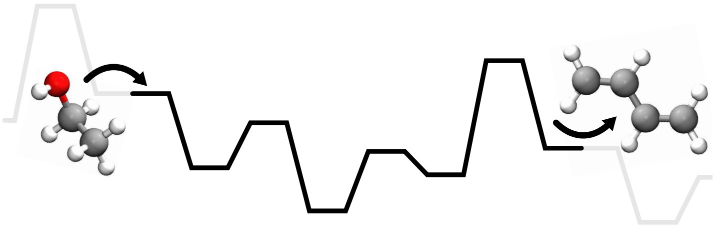

Two perspectives on first-principles based kinetic modelling

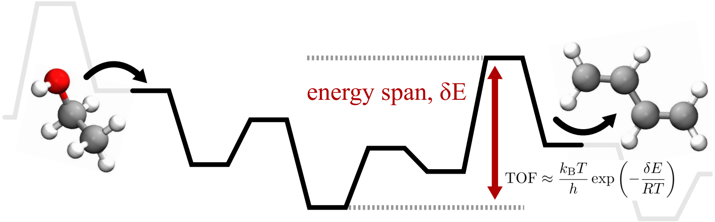

Two perspectives on first-principles based kinetic modelling

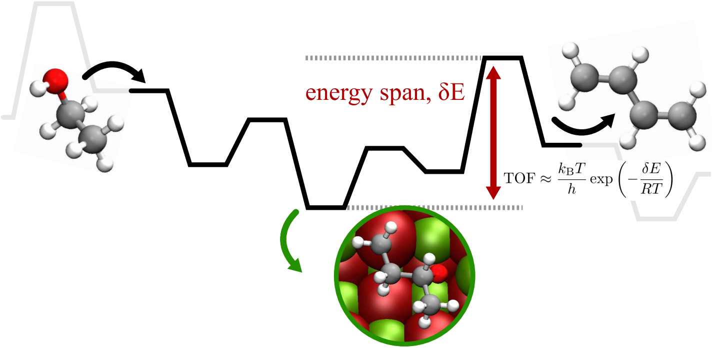

Two perspectives on first-principles based kinetic modelling

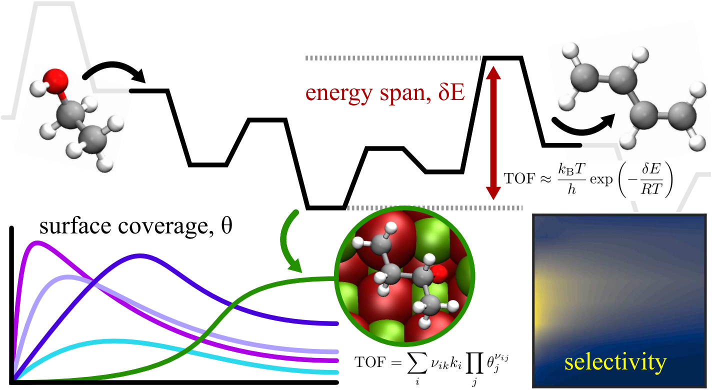

Energy span model compares pairwise energy differences

Rate determining *states* determined by identifying largest energy penalties between intermediates and transition states across catalytic cycles[1]

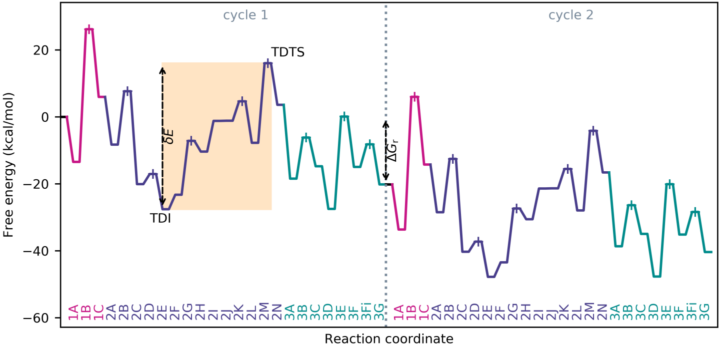

Energy landscape for ethanol dehydrogenation, aldol condensation and reduction of crotonaldehyde (723 K)[2]

[1] Kozuch and Shaik, Acc. Chem. Res., 2011, 44, 101. [2] Boje *et al.*, ChemRxiv, 2020.

Energy span model compares pairwise energy differences

Rate determining *states* determined by identifying largest energy penalties between intermediates and transition states across catalytic cycles[1]

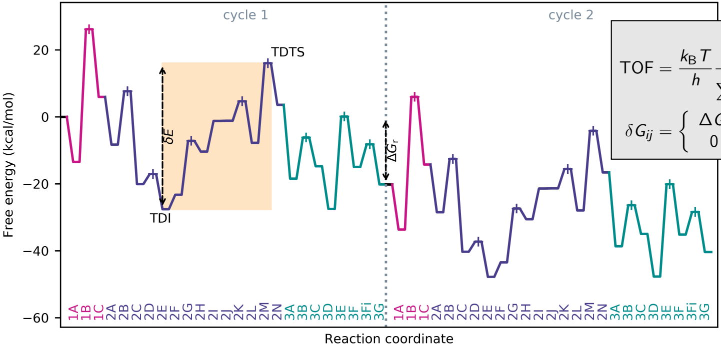

$$\mathrm{TOF} = \frac{k_\mathrm{B} T}{h} \frac{e^{-\Delta G_\mathrm{r}/RT} - 1}{\sum_{ij} e^{\left(G_{T_i} - G_{I_j} - \delta G_{ij}\right)/RT}}$$

$$\delta G_{ij} = \begin{cases} \Delta G_\mathrm{r} & i \geq j \\ 0 & i < j \end{cases}$$

Energy landscape for ethanol dehydrogenation, aldol condensation and reduction of crotonaldehyde (723 K)[2]

[1] Kozuch and Shaik, Acc. Chem. Res., 2011, 44, 101. [2] Boje *et al.*, ChemRxiv, 2020.

Energy span model compares pairwise energy differences

Rate determining *states* determined by identifying largest energy penalties between intermediates and transition states across catalytic cycles[1]

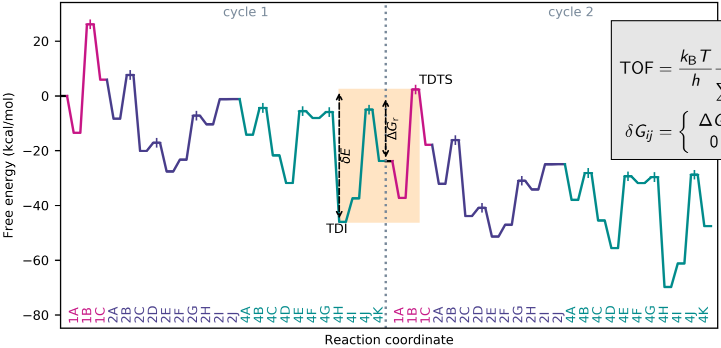

$$\mathrm{TOF} = \frac{k_B T}{h} \frac{e^{-\Delta G_r/RT} - 1}{\sum_{ij} e^{\left(G_{T_i} - G_{I_j} - \delta G_{ij}\right)/RT}}$$

$$\delta G_{ij} = \begin{cases} \Delta G_r & i \geq j \\ 0 & i < j \end{cases}$$

Energy landscape for ethanol dehydrogenation, aldol condensation and reduction of acetaldol (723 K)[2]

[1]Kozuch and Shaik, Acc. Chem. Res., 2011, 44, 101. [2]Boje *et al.*, ChemRxiv, 2020.

TOF-determining states can vary with temperature

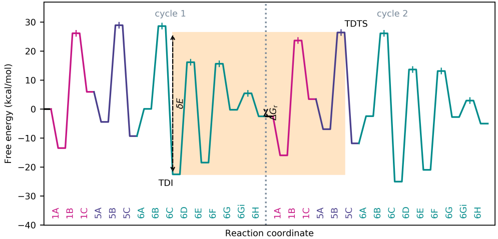

Energy landscape for ethanol dehydration pathway

Boje *et al.*, ChemRxiv, 2020.

TOF-determining states can vary with temperature

accounting for temperature
in entropy contributions
to free energy

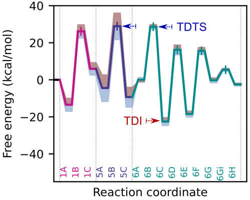

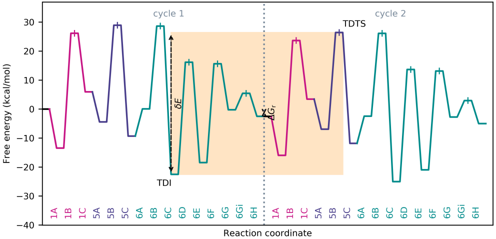

Energy landscape for ethanol dehydration pathway

Boje *et al.*, ChemRxiv, 2020.

TOF-determining states can vary with temperature

accounting for temperature in entropy contributions to free energy

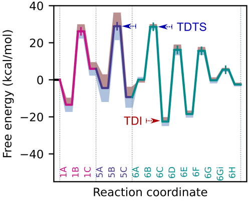

rate determining states vary with temperature

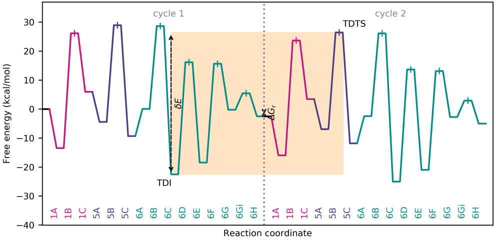

Energy landscape for ethanol dehydration pathway

Boje *et al.*, ChemRxiv, 2020.

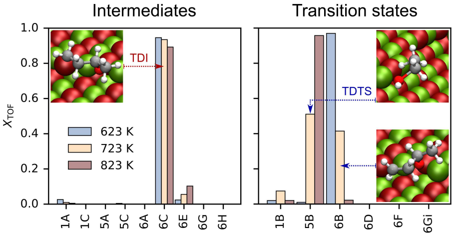

Degree of turnover frequency control

TOF-determining states can vary with temperature

accounting for temperature
in entropy contributions
to free energy

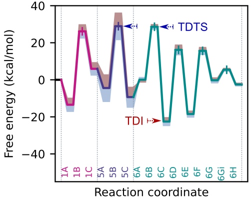

$$X_{\mathrm{TOF,T}_i} = \frac{\sum_j e^{\left(G_{T_i} - G_{I_j} - \delta G_{ij}\right)/RT}}{\sum_{ij} e^{\left(G_{T_i} - G_{I_j} - \delta G_{ij}\right)/RT}}$$

$$X_{\mathrm{TOF,I}_j} = \frac{\sum_i e^{\left(G_{T_i} - G_{I_j} - \delta G_{ij}\right)/RT}}{\sum_{ij} e^{\left(G_{T_i} - G_{I_j} - \delta G_{ij}\right)/RT}}$$

rate determining states vary with temperature

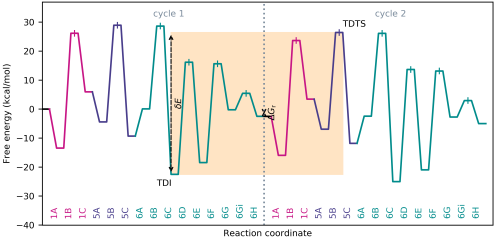

Energy landscape for ethanol dehydration pathway

Boje *et al.*, ChemRxiv, 2020.

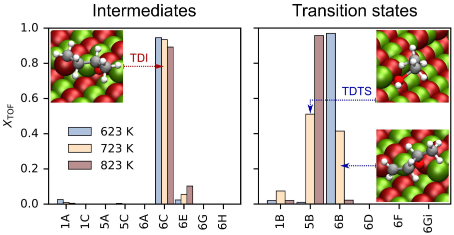

Degree of turnover frequency control

Two-carbon and four-carbon states were found to be most important

TOF-determining states for each pathway

Sequence	Intermediate	Transition state	
p123	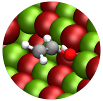 C=CO	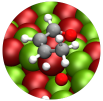 CCCC=O	
p124	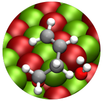 C=CCCO	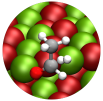 CC=O	
p156	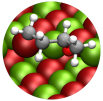 CC(O)CC	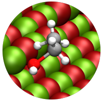 CCO	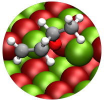 CC(O)CC

Boje *et al.*, ChemRxiv, 2020.

Energy span model estimates maximum theoretical turnover

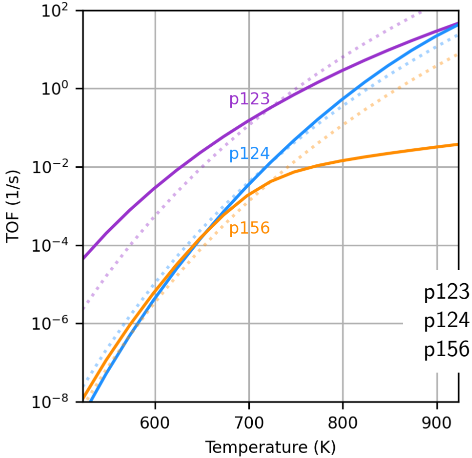

Energy spans

Sequence	δE (kcal mol^{-1}) 623 K	723 K	823 K
p123	41.9	43.6	45.3
p124	49.2	48.4	47.5
p156	48.9	49.0	54.5

p123 Dehydrogenation, aldol condensation, reduction (CA)
p124 Dehydrogenation, aldol condensation, reduction (AA)
p156 Dehydration, Prins condensation

Boje *et al.*, ChemRxiv, 2020.

Energy span model estimates maximum theoretical turnover

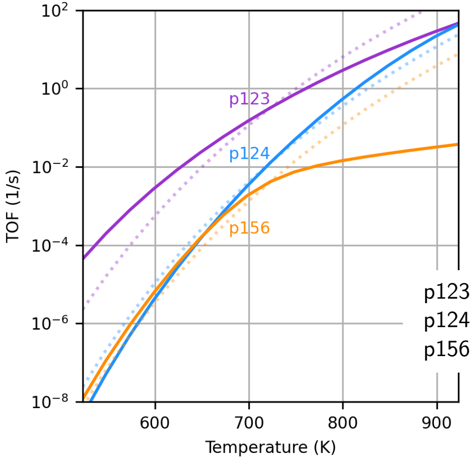

These results do not account for:

p123	Dehydrogenation, aldol condensation, reduction (CA)
p124	Dehydrogenation, aldol condensation, reduction (AA)
p156	Dehydration, Prins condensation

Boje *et al.*, ChemRxiv, 2020.

Energy span model estimates maximum theoretical turnover

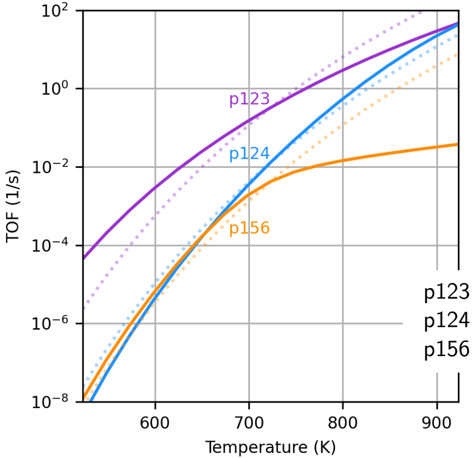

These results do not account for:

- Concentrations or surface coverage

p123	Dehydrogenation, aldol condensation, reduction (CA)
p124	Dehydrogenation, aldol condensation, reduction (AA)
p156	Dehydration, Prins condensation

Boje *et al.*, ChemRxiv, 2020.

Energy span model estimates maximum theoretical turnover

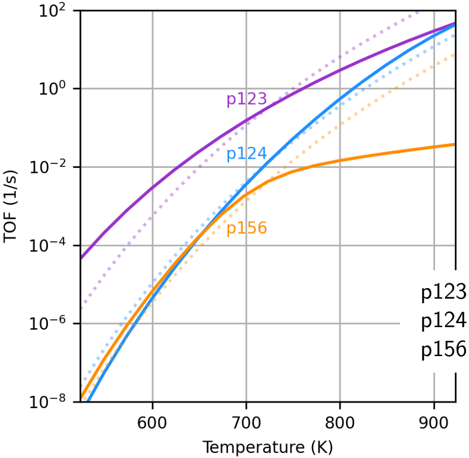

These results do not account for:

- Concentrations or surface coverage
- Competition between pathways

p123	Dehydrogenation, aldol condensation, reduction (CA)
p124	Dehydrogenation, aldol condensation, reduction (AA)
p156	Dehydration, Prins condensation

Boje *et al.*, ChemRxiv, 2020.

Constituents of the microkinetic model for ethanol-to-butadiene

	Path	Reaction	Net rate
1	1A–C	$C_2H_5O + H \leftrightarrow C_2H_4O + H_{2(g)}$	$r_1 = k_1^f \theta_{C_2H_5O}\theta_H - k_1^r p_{H_2}\theta_{C_2H_4O}\theta_*$
2	2A–C	$C_2H_4O \leftrightarrow C_2H_3O + H$	$r_2 = k_2^f \theta_{C_2H_4O}\theta_* - k_2^r \theta_{C_2H_3O}\theta_H$
3	2F–H	$C_2H_3O + C_2H_4O \leftrightarrow C_4H_7O_2$	$r_3 = k_3^f \theta_{C_2H_3O}\theta_{C_2H_4O} - k_3^r \theta_{C_4H_7O_2}\theta_*$
4	2J–L	$C_4H_7O_2 \leftrightarrow C_4H_6O_2 + H$	$r_4 = k_4^f \theta_{C_4H_7O_2}\theta_* - k_4^r \theta_{C_4H_6O_2}\theta_H$
5	2L–N	$C_4H_6O_2 \leftrightarrow C_4H_6O^{i_1} + O$	$r_5 = k_5^f \theta_{C_4H_6O_2}\theta_* - k_5^r \theta_{C_4H_6O^{i_1}}\theta_O$
6	3A–C	$C_2H_5O + C_4H_6O^{i_1} \leftrightarrow C_2H_4O + C_4H_7O^{i_1}$	$r_6 = k_6^f \theta_{C_2H_5O}\theta_{C_4H_6O^{i_1}} - k_6^r \theta_{C_2H_4O}\theta_{C_4H_7O^{i_1}}$
7	3D–F	$C_4H_7O^{i_1} \leftrightarrow C_4H_6O^{i_2} + H$	$r_7 = k_7^f \theta_{C_4H_7O^{i_1}}\theta_* - k_7^r \theta_{C_4H_6O^{i_2}}\theta_H$
8	3F–G	$C_4H_6O^{i_2} \leftrightarrow O + C_4H_{6(g)}$	$r_8 = k_8^f \theta_{C_4H_6O^{i_2}} - k_8^r p_{C_4H_6}\theta_O$
9	4A–C	$C_2H_5O + C_4H_7O_2 \leftrightarrow C_2H_4O + C_4H_8O_2{}^{i_1}$	$r_9 = k_9^f \theta_{C_2H_5O}\theta_{C_4H_7O_2} - k_9^r \theta_{C_2H_4O}\theta_{C_4H_8O_2{}^{i_1}}$
10	4C*–D	$C_4H_8O_2{}^{i_1} + H \leftrightarrow C_4H_9O_2{}^{i_1}$	$r_{10} = k_{10}^f \theta_{C_4H_8O_2{}^{i_1}}\theta_H - k_{10}^r \theta_{C_4H_9O_2{}^{i_1}}\theta_*$
11	4D–F	$C_4H_9O_2{}^{i_1} \leftrightarrow C_4H_8O_2{}^{i_2} + H$	$r_{11} = k_{11}^f \theta_{C_4H_9O_2{}^{i_1}}\theta_* - k_{11}^r \theta_{C_4H_8O_2{}^{i_2}}\theta_H$
12	4F–H	$C_4H_8O_2{}^{i_2} \leftrightarrow C_4H_7O^{i_2} + OH$	$r_{12} = k_{12}^f \theta_{C_4H_8O_2{}^{i_2}}\theta_* - k_{12}^r \theta_{C_4H_7O^{i_2}}\theta_{OH}$
13	4I–K	$C_4H_7O^{i_2} \leftrightarrow O + H + C_4H_{6(g)}$	$r_{13} = k_{13}^f \theta_{C_4H_7O^{i_2}}\theta_* - k_{13}^r p_{C_4H_6}\theta_O\theta_H$
14	5A–C	$C_2H_5O + H \leftrightarrow OH + H + C_2H_{4(g)}$	$r_{14} = k_{14}^f \theta_{C_2H_5O}\theta_H - k_{14}^r p_{C_2H_4}\theta_{OH}\theta_H$
15	6A–C	$C_2H_4O + C_2H_{4(g)} \leftrightarrow C_4H_8O$	$r_{15} = k_{15}^f p_{C_2H_4}\theta_{C_2H_4O}\theta_* - k_{15}^r \theta_{C_4H_8O}\theta_*$
16	6C–E	$C_4H_8O \leftrightarrow C_4H_7O^{i_3} + H$	$r_{16} = k_{16}^f \theta_{C_4H_8O}\theta_* - k_{16}^r \theta_{C_4H_7O^{i_3}}\theta_H$
17	6E–G	$C_4H_7O^{i_3} \leftrightarrow C_4H_6O^{i_3} + H$	$r_{17} = k_{17}^f \theta_{C_4H_7O^{i_3}}\theta_* - k_{17}^r \theta_{C_4H_6O^{i_3}}\theta_H$
18	6G–H	$C_4H_6O^{i_3} \leftrightarrow O + C_4H_{6(g)}$	$r_{18} = k_{18}^f \theta_{C_4H_6O^{i_3}} - k_{18}^r p_{C_4H_6}\theta_O$
19	7A–E	$C_2H_4O + C_2H_5O \leftrightarrow C_4H_9O_2{}^{i_2}$	$r_{19} = k_{19}^f \theta_{C_2H_4O}\theta_{C_2H_5O} - k_{19}^r \theta_{C_4H_9O_2{}^{i_2}}\theta_*$
20	9C–D	$OH \leftrightarrow H + O$	$r_{20} = k_{20}^f \theta_{OH}\theta_* - k_{20}^r \theta_H\theta_O$
21	0–1A	$C_2H_5OH_{(g)} \leftrightarrow C_2H_5O + H$	$r_{21} = k_{21}^f p_{C_2H_5OH}\theta_*^2 - k_{21}^r \theta_{C_2H_5O}\theta_H$
22	8A–C	$H_{2(g)} \leftrightarrow 2H$	$r_{22} = k_{22}^f p_{H_2}\theta_*^2 - k_{22}^r \theta_H^2$
23	9A–B	$H_2O_{(g)} \leftrightarrow OH + H$	$r_{23} = k_{23}^f p_{H_2O}\theta_*^2 - k_{23}^r \theta_{OH}\theta_H$
24	10A–B	$C_2H_4O_{(g)} \leftrightarrow C_2H_4O$	$r_{24} = k_{24}^f \theta_{C_2H_4O} - k_{24}^r p_{C_2H_4O}\theta_*$
25	2O–N	$C_4H_6O_{(g)} \leftrightarrow C_4H_6O^{i_1}$	$r_{25} = k_{25}^f \theta_{C_4H_6O^{i_1}} - k_{25}^r p_{C_4H_6O}\theta_*$

Boje *et al.*, ChemRxiv, 2020.

Constituents of the microkinetic model for ethanol-to-butadiene

	Path	Reaction	Net rate
1	1A–C	$C_2H_5O + H \leftrightarrow C_2H_4O + H_{2(g)}$	$r_1 = k_1^f\theta_{C_2H_5O}\theta_H - k_1^r p_{H_2}\theta_{C_2H_4O}\theta_*$
2	2A–C	$C_2H_4O \leftrightarrow C_2H_3O + H$	$r_2 = k_2^f\theta_{C_2H_4O}\theta_* - k_2^r\theta_{C_2H_3O}\theta_H$
3	2F–H	$C_2H_3O + C_2H_4O \leftrightarrow C_4H_7O_2$	$r_3 = k_3^f\theta_{C_2H_3O}\theta_{C_2H_4O} - k_3^r\theta_{C_4H_7O_2}\theta_*$
4	2J–L	$C_4H_7O_2 \leftrightarrow C_4H_6O_2 + H$	$r_4 = k_4^f\theta_{C_4H_7O_2}\theta_* - k_4^r\theta_{C_4H_6O_2}\theta_H$
5	2L–N	$C_4H_6O_2 \leftrightarrow C_4H_6O^{i_1} + O$	$r_5 = k_5^f\theta_{C_4H_6O_2}\theta_* - k_5^r\theta_{C_4H_6O^{i_1}}\theta_O$
6	3A–C	$C_2H_5O + C_4H_6O^{i_1} \leftrightarrow C_2H_4O + C_4H_7O^{i_1}$	$r_6 = k_6^f\theta_{C_2H_5O}\theta_{C_4H_6O^{i_1}} - k_6^r\theta_{C_2H_4O}\theta_{C_4H_7O^{i_1}}$
7	3D–F	$C_4H_7O^{i_1} \leftrightarrow C_4H_6O^{i_2} + H$	$r_7 = k_7^f\theta_{C_4H_7O^{i_1}}\theta_* - k_7^r\theta_{C_4H_6O^{i_2}}\theta_H$
8	3F–G	$C_4H_6O^{i_2} \leftrightarrow O + C_4H_{6(g)}$	$r_8 = k_8^f\theta_{C_4H_6O^{i_2}} - k_8^r p_{C_4H_6}\theta_O$
9	4A–C	$C_2H_5O + C_4H_7O_2 \leftrightarrow C_2H_4O + C_4H_8O_2{}^{i_1}$	$r_9 = k_9^f\theta_{C_2H_5O}\theta_{C_4H_7O_2} - k_9^r\theta_{C_2H_4O}\theta_{C_4H_8O_2{}^{i_1}}$
10	4C*–D	$C_4H_8O_2{}^{i_1} + H \leftrightarrow C_4H_9O_2{}^{i_1}$	$r_{10} = k_{10}^f\theta_{C_4H_8O_2{}^{i_1}}\theta_H - k_{10}^r\theta_{C_4H_9O_2{}^{i_1}}\theta_*$
11	4D–F	$C_4H_9O_2{}^{i_1} \leftrightarrow C_4H_8O_2{}^{i_2} + H$	$r_{11} = k_{11}^f\theta_{C_4H_9O_2{}^{i_1}}\theta_* - k_{11}^r\theta_{C_4H_8O_2{}^{i_2}}\theta_H$
12	4F–H	$C_4H_8O_2{}^{i_2} \leftrightarrow C_4H_7O^{i_2} + OH$	$r_{12} = k_{12}^f\theta_{C_4H_8O_2{}^{i_2}}\theta_* - k_{12}^r\theta_{C_4H_7O^{i_2}}\theta_{OH}$
13	4I–K	$C_4H_7O^{i_2} \leftrightarrow O + H + C_4H_{6(g)}$	$r_{13} = k_{13}^f\theta_{C_4H_7O^{i_2}}\theta_* - k_{13}^r p_{C_4H_6}\theta_O\theta_H$
14	5A–C	$C_2H_5O + H \leftrightarrow OH + H + C_2H_{4(g)}$	$r_{14} = k_{14}^f\theta_{C_2H_5O}\theta_H - k_{14}^r p_{C_2H_4}\theta_{OH}\theta_H$
15	6A–C	$C_2H_4O + C_2H_{4(g)} \leftrightarrow C_4H_8O$	$r_{15} = k_{15}^f p_{C_2H_4}\theta_{C_2H_4O}\theta_* - k_{15}^r\theta_{C_4H_8O}\theta_*$
16	6C–E	$C_4H_8O \leftrightarrow C_4H_7O^{i_3} + H$	$r_{16} = k_{16}^f\theta_{C_4H_8O}\theta_* - k_{16}^r\theta_{C_4H_7O^{i_3}}\theta_H$
17	6E–G	$C_4H_7O^{i_3} \leftrightarrow C_4H_6O^{i_3} + H$	$r_{17} = k_{17}^f\theta_{C_4H_7O^{i_3}}\theta_* - k_{17}^r\theta_{C_4H_6O^{i_3}}\theta_H$
18	6G–H	$C_4H_6O^{i_3} \leftrightarrow O + C_4H_{6(g)}$	$r_{18} = k_{18}^f\theta_{C_4H_6O^{i_3}} - k_{18}^r p_{C_4H_6}\theta_O$
19	7A–E	$C_2H_4O + C_2H_5O \leftrightarrow C_4H_9O_2{}^{i_2}$	$r_{19} = k_{19}^f\theta_{C_2H_4O}\theta_{C_2H_5O} - k_{19}^r\theta_{C_4H_9O_2{}^{i_2}}\theta_*$
20	9C–D	$OH \leftrightarrow H + O$	$r_{20} = k_{20}^f\theta_{OH}\theta_* - k_{20}^r\theta_H\theta_O$
21	0–1A	$C_2H_5OH_{(g)} \leftrightarrow C_2H_5O + H$	$r_{21} = k_{21}^f p_{C_2H_5OH}\theta_*^2 - k_{21}^r\theta_{C_2H_5O}\theta_H$
22	8A–C	$H_{2(g)} \leftrightarrow 2H$	$r_{22} = k_{22}^f p_{H_2}\theta_*^2 - k_{22}^r\theta_H^2$
23	9A–B	$H_2O_{(g)} \leftrightarrow OH + H$	$r_{23} = k_{23}^f p_{H_2O}\theta_*^2 - k_{23}^r\theta_{OH}\theta_H$
24	10A–B	$C_2H_4O_{(g)} \leftrightarrow C_2H_4O$	$r_{24} = k_{24}^f\theta_{C_2H_4O} - k_{24}^r p_{C_2H_4O}\theta_*$
25	2O–N	$C_4H_6O_{(g)} \leftrightarrow C_4H_6O^{i_1}$	$r_{25} = k_{25}^f\theta_{C_4H_6O^{i_1}} - k_{25}^r p_{C_4H_6O}\theta_*$

Arrhenius rate constants:

$$k^f = \frac{k_B T}{h}\exp\left(-\frac{\Delta G_a}{RT}\right)$$

$$\Delta G_a = G_{TS} - G_{IS}$$

Boje *et al.*, ChemRxiv, 2020.

Constituents of the microkinetic model for ethanol-to-butadiene

	Path	Reaction	Net rate
1	1A–C	$C_2H_5O + H \leftrightarrow C_2H_4O + H_{2(g)}$	$r_1 = k_1^f\theta_{C_2H_5O}\theta_H - k_1^r p_{H_2}\theta_{C_2H_4O}\theta_*$
2	2A–C	$C_2H_4O \leftrightarrow C_2H_3O + H$	$r_2 = k_2^f\theta_{C_2H_4O}\theta_* - k_2^r\theta_{C_2H_3O}\theta_H$
3	2F–H	$C_2H_3O + C_2H_4O \leftrightarrow C_4H_7O_2$	$r_3 = k_3^f\theta_{C_2H_3O}\theta_{C_2H_4O} - k_3^r\theta_{C_4H_7O_2}\theta_*$
4	2J–L	$C_4H_7O_2 \leftrightarrow C_4H_6O_2 + H$	$r_4 = k_4^f\theta_{C_4H_7O_2}\theta_* - k_4^r\theta_{C_4H_6O_2}\theta_H$
5	2L–N	$C_4H_6O_2 \leftrightarrow C_4H_6O^{i_1} + O$	$r_5 = k_5^f\theta_{C_4H_6O_2}\theta_* - k_5^r\theta_{C_4H_6O^{i_1}}\theta_O$
6	3A–C	$C_2H_5O + C_4H_6O^{i_1} \leftrightarrow C_2H_4O + C_4H_7O^{i_1}$	$r_6 = k_6^f\theta_{C_2H_5O}\theta_{C_4H_6O^{i_1}} - k_6^r\theta_{C_2H_4O}\theta_{C_4H_7O^{i_1}}$
7	3D–F	$C_4H_7O^{i_1} \leftrightarrow C_4H_6O^{i_2} + H$	$r_7 = k_7^f\theta_{C_4H_7O^{i_1}}\theta_* - k_7^r\theta_{C_4H_6O^{i_2}}\theta_H$
8	3F–G	$C_4H_6O^{i_2} \leftrightarrow O + C_4H_{6(g)}$	$r_8 = k_8^f\theta_{C_4H_6O^{i_2}} - k_8^r p_{C_4H_6}\theta_O$
9	4A–C	$C_2H_5O + C_4H_7O_2 \leftrightarrow C_2H_4O + C_4H_8O_2{}^{i_1}$	$r_9 = k_9^f\theta_{C_2H_5O}\theta_{C_4H_7O_2} - k_9^r\theta_{C_2H_4O}\theta_{C_4H_8O_2{}^{i_1}}$
10	4C*–D	$C_4H_8O_2{}^{i_1} + H \leftrightarrow C_4H_9O_2{}^{i_1}$	$r_{10} = k_{10}^f\theta_{C_4H_8O_2{}^{i_1}}\theta_H - k_{10}^r\theta_{C_4H_9O_2{}^{i_1}}\theta_*$
11	4D–F	$C_4H_9O_2{}^{i_1} \leftrightarrow C_4H_8O_2{}^{i_2} + H$	$r_{11} = k_{11}^f\theta_{C_4H_9O_2{}^{i_1}}\theta_* - k_{11}^r\theta_{C_4H_8O_2{}^{i_2}}\theta_H$
12	4F–H	$C_4H_8O_2{}^{i_2} \leftrightarrow C_4H_7O^{i_2} + OH$	$r_{12} = k_{12}^f\theta_{C_4H_8O_2{}^{i_2}}\theta_* - k_{12}^r\theta_{C_4H_7O^{i_2}}\theta_{OH}$
13	4I–K	$C_4H_7O^{i_2} \leftrightarrow O + H + C_4H_{6(g)}$	$r_{13} = k_{13}^f\theta_{C_4H_7O^{i_2}}\theta_* - k_{13}^r p_{C_4H_6}\theta_O\theta_H$
14	5A–C	$C_2H_5O + H \leftrightarrow OH + H + C_2H_{4(g)}$	$r_{14} = k_{14}^f\theta_{C_2H_5O}\theta_H - k_{14}^r p_{C_2H_4}\theta_{OH}\theta_H$
15	6A–C	$C_2H_4O + C_2H_{4(g)} \leftrightarrow C_4H_8O$	$r_{15} = k_{15}^f p_{C_2H_4}\theta_{C_2H_4O}\theta_* - k_{15}^r\theta_{C_4H_8O}\theta_*$
16	6C–E	$C_4H_8O \leftrightarrow C_4H_7O^{i_3} + H$	$r_{16} = k_{16}^f\theta_{C_4H_8O}\theta_* - k_{16}^r\theta_{C_4H_7O^{i_3}}\theta_H$
17	6E–G	$C_4H_7O^{i_3} \leftrightarrow C_4H_6O^{i_3} + H$	$r_{17} = k_{17}^f\theta_{C_4H_7O^{i_3}}\theta_* - k_{17}^r\theta_{C_4H_6O^{i_3}}\theta_H$
18	6G–H	$C_4H_6O^{i_3} \leftrightarrow O + C_4H_{6(g)}$	$r_{18} = k_{18}^f\theta_{C_4H_6O^{i_3}} - k_{18}^r p_{C_4H_6}\theta_O$
19	7A–E	$C_2H_4O + C_2H_5O \leftrightarrow C_4H_9O_2{}^{i_2}$	$r_{19} = k_{19}^f\theta_{C_2H_4O}\theta_{C_2H_5O} - k_{19}^r\theta_{C_4H_9O_2{}^{i_2}}\theta_*$
20	9C–D	$OH \leftrightarrow H + O$	$r_{20} = k_{20}^f\theta_{OH}\theta_* - k_{20}^r\theta_H\theta_O$
21	0–1A	$C_2H_5OH_{(g)} \leftrightarrow C_2H_5O + H$	$r_{21} = k_{21}^f p_{C_2H_5OH}\theta_*^2 - k_{21}^r\theta_{C_2H_5O}\theta_H$
22	8A–C	$H_{2(g)} \leftrightarrow 2H$	$r_{22} = k_{22}^f p_{H_2}\theta_*^2 - k_{22}^r\theta_H^2$
23	9A–B	$H_2O_{(g)} \leftrightarrow OH + H$	$r_{23} = k_{23}^f p_{H_2O}\theta_*^2 - k_{23}^r\theta_{OH}\theta_H$
24	10A–B	$C_2H_4O_{(g)} \leftrightarrow C_2H_4O$	$r_{24} = k_{24}^f\theta_{C_2H_4O} - k_{24}^r p_{C_2H_4O}\theta_*$
25	2O–N	$C_4H_6O_{(g)} \leftrightarrow C_4H_6O^{i_1}$	$r_{25} = k_{25}^f\theta_{C_4H_6O^{i_1}} - k_{25}^r p_{C_4H_6O}\theta_*$

Arrhenius rate constants:

$$k^f = \frac{k_B T}{h}\exp\left(-\frac{\Delta G_a}{RT}\right)$$

$$\Delta G_a = G_{TS} - G_{IS}$$

Adsorption rate constants:

$$k^f = \frac{A}{\sqrt{2\pi M k_B T}}$$

Boje *et al.*, ChemRxiv, 2020.

Constituents of the microkinetic model for ethanol-to-butadiene

	Path	Reaction	Net rate
1	1A–C	$C_2H_5O + H \leftrightarrow C_2H_4O + H_{2(g)}$	$r_1 = k_1^f \theta_{C_2H_5O}\theta_H - k_1^r p_{H_2}\theta_{C_2H_4O}\theta_*$
2	2A–C	$C_2H_4O \leftrightarrow C_2H_3O + H$	$r_2 = k_2^f \theta_{C_2H_4O}\theta_* - k_2^r \theta_{C_2H_3O}\theta_H$
3	2F–H	$C_2H_3O + C_2H_4O \leftrightarrow C_4H_7O_2$	$r_3 = k_3^f \theta_{C_2H_3O}\theta_{C_2H_4O} - k_3^r \theta_{C_4H_7O_2}\theta_*$
4	2J–L	$C_4H_7O_2 \leftrightarrow C_4H_6O_2 + H$	$r_4 = k_4^f \theta_{C_4H_7O_2}\theta_* - k_4^r \theta_{C_4H_6O_2}\theta_H$
5	2L–N	$C_4H_6O_2 \leftrightarrow C_4H_6O^{i_1} + O$	$r_5 = k_5^f \theta_{C_4H_6O_2}\theta_* - k_5^r \theta_{C_4H_6O^{i_1}}\theta_O$
6	3A–C	$C_2H_5O + C_4H_6O^{i_1} \leftrightarrow C_2H_4O + C_4H_7O^{i_1}$	$r_6 = k_6^f \theta_{C_2H_5O}\theta_{C_4H_6O^{i_1}} - k_6^r \theta_{C_2H_4O}\theta_{C_4H_7O^{i_1}}$
7	3D–F	$C_4H_7O^{i_1} \leftrightarrow C_4H_6O^{i_2} + H$	$r_7 = k_7^f \theta_{C_4H_7O^{i_1}}\theta_* - k_7^r \theta_{C_4H_6O^{i_2}}\theta_H$
8	3F–G	$C_4H_6O^{i_2} \leftrightarrow O + C_4H_{6(g)}$	$r_8 = k_8^f \theta_{C_4H_6O^{i_2}} - k_8^r p_{C_4H_6}\theta_O$
9	4A–C	$C_2H_5O + C_4H_7O_2 \leftrightarrow C_2H_4O + C_4H_8O_2{}^{i_1}$	$r_9 = k_9^f \theta_{C_2H_5O}\theta_{C_4H_7O_2} - k_9^r \theta_{C_2H_4O}\theta_{C_4H_8O_2{}^{i_1}}$
10	4C*–D	$C_4H_8O_2{}^{i_1} + H \leftrightarrow C_4H_9O_2{}^{i_1}$	$r_{10} = k_{10}^f \theta_{C_4H_8O_2{}^{i_1}}\theta_H - k_{10}^r \theta_{C_4H_9O_2{}^{i_1}}\theta_*$
11	4D–F	$C_4H_9O_2{}^{i_1} \leftrightarrow C_4H_8O_2{}^{i_2} + H$	$r_{11} = k_{11}^f \theta_{C_4H_9O_2{}^{i_1}}\theta_* - k_{11}^r \theta_{C_4H_8O_2{}^{i_2}}\theta_H$
12	4F–H	$C_4H_8O_2{}^{i_2} \leftrightarrow C_4H_7O^{i_2} + OH$	$r_{12} = k_{12}^f \theta_{C_4H_8O_2{}^{i_2}}\theta_* - k_{12}^r \theta_{C_4H_7O^{i_2}}\theta_{OH}$
13	4I–K	$C_4H_7O^{i_2} \leftrightarrow O + H + C_4H_{6(g)}$	$r_{13} = k_{13}^f \theta_{C_4H_7O^{i_2}}\theta_* - k_{13}^r p_{C_4H_6}\theta_O\theta_H$
14	5A–C	$C_2H_5O + H \leftrightarrow OH + H + C_2H_{4(g)}$	$r_{14} = k_{14}^f \theta_{C_2H_5O}\theta_H - k_{14}^r p_{C_2H_4}\theta_{OH}\theta_H$
15	6A–C	$C_2H_4O + C_2H_{4(g)} \leftrightarrow C_4H_8O$	$r_{15} = k_{15}^f p_{C_2H_4}\theta_{C_2H_4O}\theta_* - k_{15}^r \theta_{C_4H_8O}\theta_*$
16	6C–E	$C_4H_8O \leftrightarrow C_4H_7O^{i_3} + H$	$r_{16} = k_{16}^f \theta_{C_4H_8O}\theta_* - k_{16}^r \theta_{C_4H_7O^{i_3}}\theta_H$
17	6E–G	$C_4H_7O^{i_3} \leftrightarrow C_4H_6O^{i_3} + H$	$r_{17} = k_{17}^f \theta_{C_4H_7O^{i_3}}\theta_* - k_{17}^r \theta_{C_4H_6O^{i_3}}\theta_H$
18	6G–H	$C_4H_6O^{i_3} \leftrightarrow O + C_4H_{6(g)}$	$r_{18} = k_{18}^f \theta_{C_4H_6O^{i_3}} - k_{18}^r p_{C_4H_6}\theta_O$
19	7A–E	$C_2H_4O + C_2H_5O \leftrightarrow C_4H_9O_2{}^{i_2}$	$r_{19} = k_{19}^f \theta_{C_2H_4O}\theta_{C_2H_5O} - k_{19}^r \theta_{C_4H_9O_2{}^{i_2}}\theta_*$
20	9C–D	$OH \leftrightarrow H + O$	$r_{20} = k_{20}^f \theta_{OH}\theta_* - k_{20}^r \theta_H\theta_O$
21	0–1A	$C_2H_5OH_{(g)} \leftrightarrow C_2H_5O + H$	$r_{21} = k_{21}^f p_{C_2H_5OH}\theta_*^2 - k_{21}^r \theta_{C_2H_5O}\theta_H$
22	8A–C	$H_{2(g)} \leftrightarrow 2H$	$r_{22} = k_{22}^f p_{H_2}\theta_*^2 - k_{22}^r \theta_H^2$
23	9A–B	$H_2O_{(g)} \leftrightarrow OH + H$	$r_{23} = k_{23}^f p_{H_2O}\theta_*^2 - k_{23}^r \theta_{OH}\theta_H$
24	10A–B	$C_2H_4O_{(g)} \leftrightarrow C_2H_4O$	$r_{24} = k_{24}^f \theta_{C_2H_4O} - k_{24}^r p_{C_2H_4O}\theta_*$
25	2O–N	$C_4H_6O_{(g)} \leftrightarrow C_4H_6O^{i_1}$	$r_{25} = k_{25}^f \theta_{C_4H_6O^{i_1}} - k_{25}^r p_{C_4H_6O}\theta_*$

Arrhenius rate constants:

$$k^f = \frac{k_B T}{h} \exp\left(-\frac{\Delta G_a}{RT}\right)$$

$$\Delta G_a = G_{TS} - G_{IS}$$

Adsorption rate constants:

$$k^f = \frac{A}{\sqrt{2\pi M k_B T}}$$

Thermodynamic consistency:

$$k^r = k^f \cdot K_{eq}^{-1}$$

$$K_{eq} = \exp\left(-\frac{\Delta G_r}{RT}\right)$$

$$\Delta G_r = G_{FS} - G_{IS}$$

Boje *et al.*, ChemRxiv, 2020.

Constituents of the microkinetic model for ethanol-to-butadiene

	Path	Reaction	Net rate
1	1A–C	$C_2H_5O + H \leftrightarrow C_2H_4O + H_{2(g)}$	$r_1 = k_1^f \theta_{C_2H_5O}\theta_H - k_1^r p_{H_2}\theta_{C_2H_4O}\theta_*$
2	2A–C	$C_2H_4O \leftrightarrow C_2H_3O + H$	$r_2 = k_2^f \theta_{C_2H_4O}\theta_* - k_2^r \theta_{C_2H_3O}\theta_H$
3	2F–H	$C_2H_3O + C_2H_4O \leftrightarrow C_4H_7O_2$	$r_3 = k_3^f \theta_{C_2H_3O}\theta_{C_2H_4O} - k_3^r \theta_{C_4H_7O_2}\theta_*$
4	2J–L	$C_4H_7O_2 \leftrightarrow C_4H_6O_2 + H$	$r_4 = k_4^f \theta_{C_4H_7O_2}\theta_* - k_4^r \theta_{C_4H_6O_2}\theta_H$
5	2L–N	$C_4H_6O_2 \leftrightarrow C_4H_6O^{i_1} + O$	$r_5 = k_5^f \theta_{C_4H_6O_2}\theta_* - k_5^r \theta_{C_4H_6O^{i_1}}\theta_O$
6	3A–C	$C_2H_5O + C_4H_6O^{i_1} \leftrightarrow C_2H_4O + C_4H_7O^{i_1}$	$r_6 = k_6^f \theta_{C_2H_5O}\theta_{C_4H_6O^{i_1}} - k_6^r \theta_{C_2H_4O}\theta_{C_4H_7O^{i_1}}$
7	3D–F	$C_4H_7O^{i_1} \leftrightarrow C_4H_6O^{i_2} + H$	$r_7 = k_7^f \theta_{C_4H_7O^{i_1}}\theta_* - k_7^r \theta_{C_4H_6O^{i_2}}\theta_H$
8	3F–G	$C_4H_6O^{i_2} \leftrightarrow O + C_4H_{6(g)}$	$r_8 = k_8^f \theta_{C_4H_6O^{i_2}} - k_8^r p_{C_4H_6}\theta_O$
9	4A–C	$C_2H_5O + C_4H_7O_2 \leftrightarrow C_2H_4O + C_4H_8O_2{}^{i_1}$	$r_9 = k_9^f \theta_{C_2H_5O}\theta_{C_4H_7O_2} - k_9^r \theta_{C_2H_4O}\theta_{C_4H_8O_2{}^{i_1}}$
10	4C*–D	$C_4H_8O_2{}^{i_1} + H \leftrightarrow C_4H_9O_2{}^{i_1}$	$r_{10} = k_{10}^f \theta_{C_4H_8O_2{}^{i_1}}\theta_H - k_{10}^r \theta_{C_4H_9O_2{}^{i_1}}\theta_*$
11	4D–F	$C_4H_9O_2{}^{i_1} \leftrightarrow C_4H_8O_2{}^{i_2} + H$	$r_{11} = k_{11}^f \theta_{C_4H_9O_2{}^{i_1}}\theta_* - k_{11}^r \theta_{C_4H_8O_2{}^{i_2}}\theta_H$
12	4F–H	$C_4H_8O_2{}^{i_2} \leftrightarrow C_4H_7O^{i_2} + OH$	$r_{12} = k_{12}^f \theta_{C_4H_8O_2{}^{i_2}}\theta_* - k_{12}^r \theta_{C_4H_7O^{i_2}}\theta_{OH}$
13	4I–K	$C_4H_7O^{i_2} \leftrightarrow O + H + C_4H_{6(g)}$	$r_{13} = k_{13}^f \theta_{C_4H_7O^{i_2}}\theta_* - k_{13}^r p_{C_4H_6}\theta_O\theta_H$
14	5A–C	$C_2H_5O + H \leftrightarrow OH + H + C_2H_{4(g)}$	$r_{14} = k_{14}^f \theta_{C_2H_5O}\theta_H - k_{14}^r p_{C_2H_4}\theta_{OH}\theta_H$
15	6A–C	$C_2H_4O + C_2H_{4(g)} \leftrightarrow C_4H_8O$	$r_{15} = k_{15}^f p_{C_2H_4}\theta_{C_2H_4O}\theta_* - k_{15}^r \theta_{C_4H_8O}\theta_*$
16	6C–E	$C_4H_8O \leftrightarrow C_4H_7O^{i_3} + H$	$r_{16} = k_{16}^f \theta_{C_4H_8O}\theta_* - k_{16}^r \theta_{C_4H_7O^{i_3}}\theta_H$
17	6E–G	$C_4H_7O^{i_3} \leftrightarrow C_4H_6O^{i_3} + H$	$r_{17} = k_{17}^f \theta_{C_4H_7O^{i_3}}\theta_* - k_{17}^r \theta_{C_4H_6O^{i_3}}\theta_H$
18	6G–H	$C_4H_6O^{i_3} \leftrightarrow O + C_4H_{6(g)}$	$r_{18} = k_{18}^f \theta_{C_4H_6O^{i_3}} - k_{18}^r p_{C_4H_6}\theta_O$
19	7A–E	$C_2H_4O + C_2H_5O \leftrightarrow C_4H_9O_2{}^{i_2}$	$r_{19} = k_{19}^f \theta_{C_2H_4O}\theta_{C_2H_5O} - k_{19}^r \theta_{C_4H_9O_2{}^{i_2}}\theta_*$
20	9C–D	$OH \leftrightarrow H + O$	$r_{20} = k_{20}^f \theta_{OH}\theta_* - k_{20}^r \theta_H\theta_O$
21	0–1A	$C_2H_5OH_{(g)} \leftrightarrow C_2H_5O + H$	$r_{21} = k_{21}^f p_{C_2H_5OH}\theta_*^2 - k_{21}^r \theta_{C_2H_5O}\theta_H$
22	8A–C	$H_{2(g)} \leftrightarrow 2H$	$r_{22} = k_{22}^f p_{H_2}\theta_*^2 - k_{22}^r \theta_H^2$
23	9A–B	$H_2O_{(g)} \leftrightarrow OH + H$	$r_{23} = k_{23}^f p_{H_2O}\theta_*^2 - k_{23}^r \theta_{OH}\theta_H$
24	10A–B	$C_2H_4O_{(g)} \leftrightarrow C_2H_4O$	$r_{24} = k_{24}^f \theta_{C_2H_4O} - k_{24}^r p_{C_2H_4O}\theta_*$
25	2O–N	$C_4H_6O_{(g)} \leftrightarrow C_4H_6O^{i_1}$	$r_{25} = k_{25}^f \theta_{C_4H_6O^{i_1}} - k_{25}^r p_{C_4H_6O}\theta_*$

Solved in MATLAB R2018a with:

- *ode23s* using BDF as the integrator
- *fsolve* as the steady state solver
- Jacobian function supplied

Boje *et al.*, ChemRxiv, 2020.

Microkinetic model enables surface coverage considerations

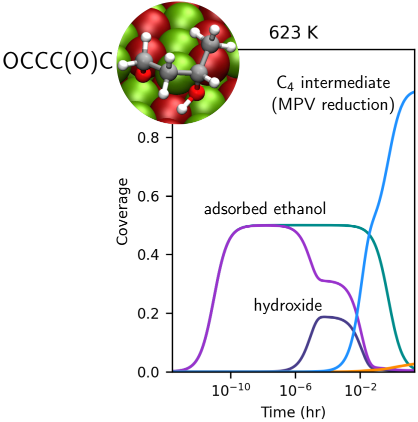

Surface coverage of dominant species over 24 hr period* as a function of temperature.
2 kPa ethanol with 1% H_2, 1% C_2H_4 and trace other products at 1 bar total pressure.

Boje *et al.*, ChemRxiv, 2020.

*Despite appearances, steady state to a reasonable tolerance

Microkinetic model enables surface coverage considerations

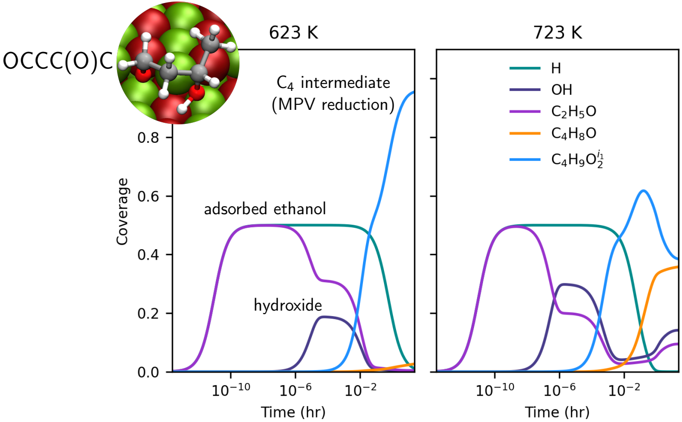

Surface coverage of dominant species over 24 hr period* as a function of temperature.
2 kPa ethanol with 1% H_2, 1% C_2H_4 and trace other products at 1 bar total pressure.

Boje *et al.*, ChemRxiv, 2020.

*Despite appearances, steady state to a reasonable tolerance

Microkinetic model enables surface coverage considerations

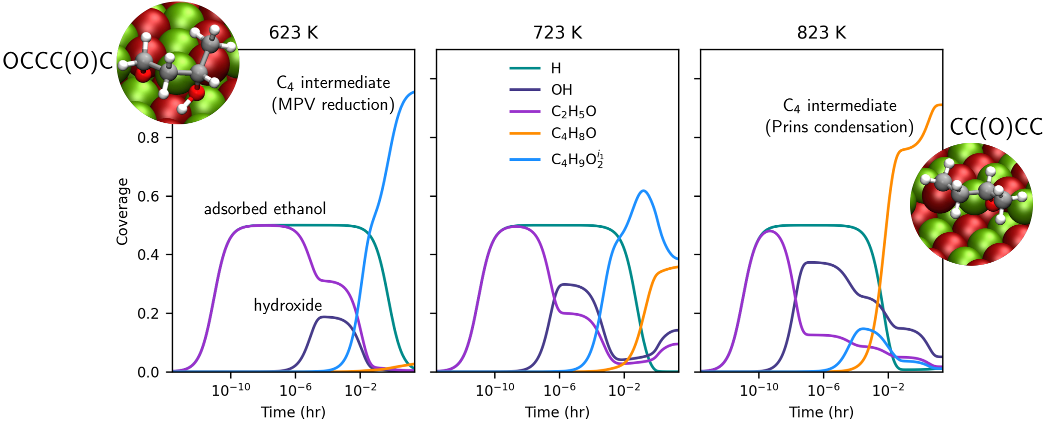

Surface coverage of dominant species over 24 hr period* as a function of temperature.
2 kPa ethanol with 1% H_2, 1% C_2H_4 and trace other products at 1 bar total pressure.

Boje *et al.*, ChemRxiv, 2020.

*Despite appearances, steady state to a reasonable tolerance

Microkinetic model predicts lower turnover

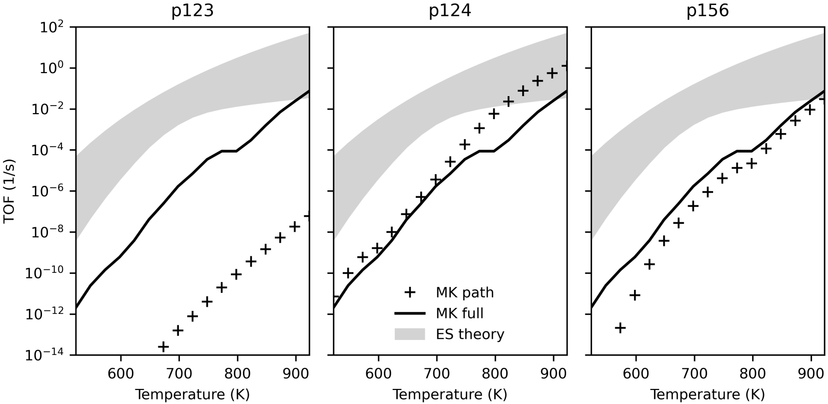

TOF predictions from ES theory (fill), full MK model (line) and pathwise MK model (markers).
2 kPa ethanol with 1% H_2, 1% C_2H_4 and trace other products at 1 bar total pressure.

Boje *et al.*, ChemRxiv, 2020.

Microkinetic model predicts lower turnover

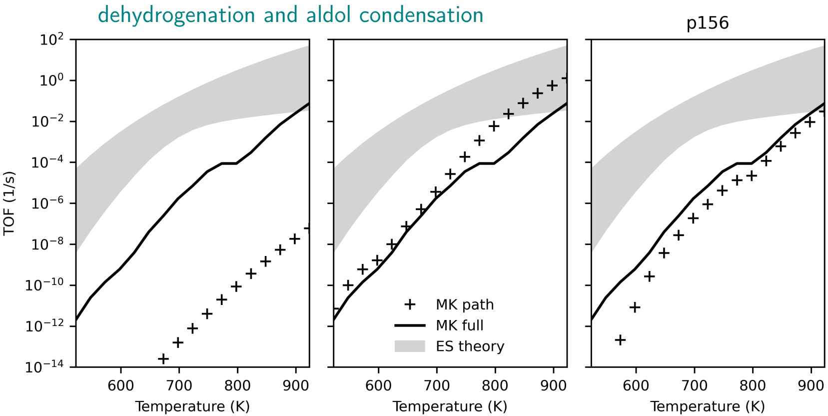

TOF predictions from ES theory (fill), full MK model (line) and pathwise MK model (markers).
2 kPa ethanol with 1% H_2, 1% C_2H_4 and trace other products at 1 bar total pressure.

Boje *et al.*, ChemRxiv, 2020.

Microkinetic model predicts lower turnover

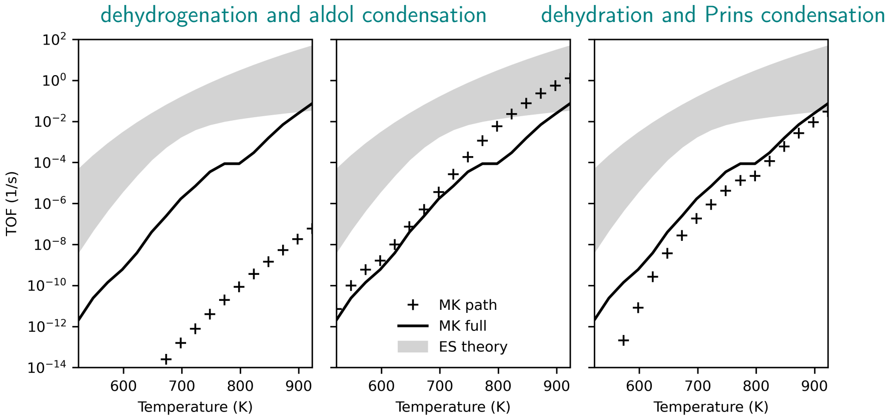

TOF predictions from ES theory (fill), full MK model (line) and pathwise MK model (markers).
2 kPa ethanol with 1% H_2, 1% C_2H_4 and trace other products at 1 bar total pressure.

Boje *et al.*, ChemRxiv, 2020.

Microkinetic model predicts lower turnover

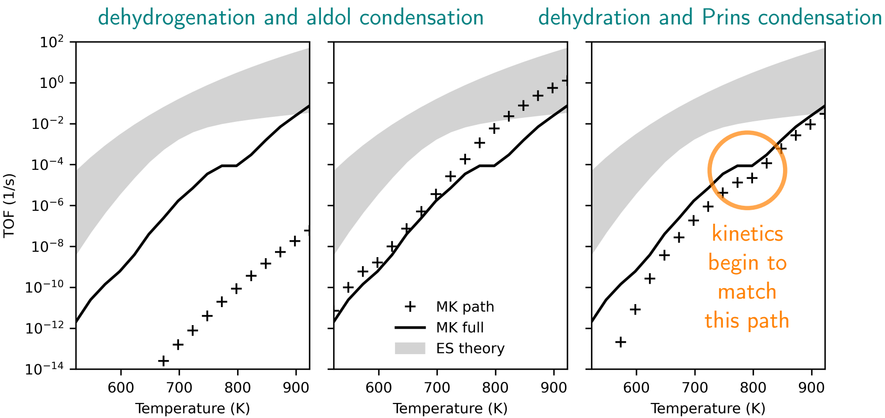

TOF predictions from ES theory (fill), full MK model (line) and pathwise MK model (markers).
2 kPa ethanol with 1% H_2, 1% C_2H_4 and trace other products at 1 bar total pressure.

Boje *et al.*, ChemRxiv, 2020.

Butadiene selectivity is also an important consideration

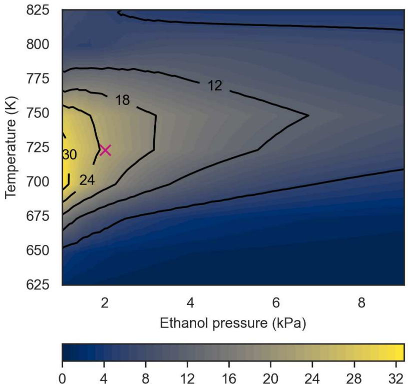

Butadiene selectivity as a function of ethanol partial pressure and temperature.
Pink cross marks typical experimental conditions.

Boje *et al.*, ChemRxiv, 2020.

Butadiene selectivity is highest where acetaldehyde selectivity is low

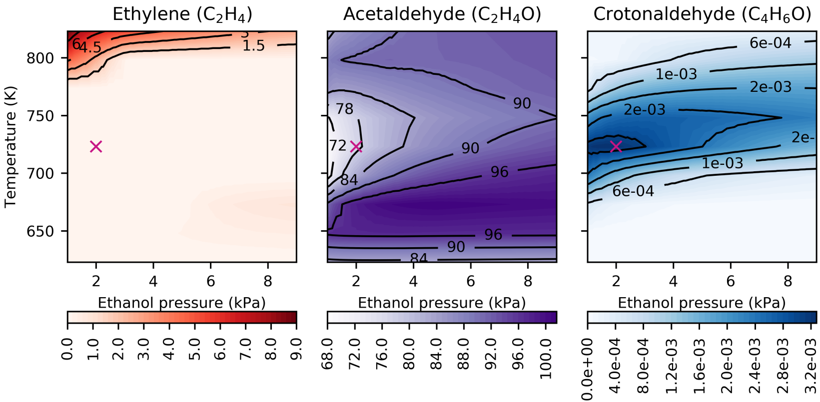

By-product selectivity as a function of ethanol partial pressure and temperature.
Pink cross marks typical experimental conditions.

Boje *et al.*, ChemRxiv, 2020.

How much should we trust the model results?

How much should we trust the model results?

Here we consider uncertainty in the DFT calculations...

How much should we trust the model results?

Here we consider uncertainty in the DFT calculations...

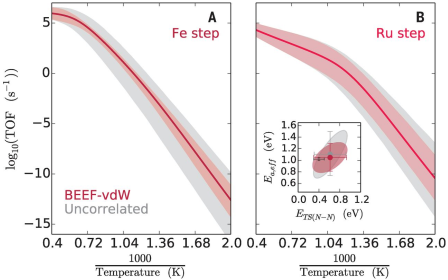

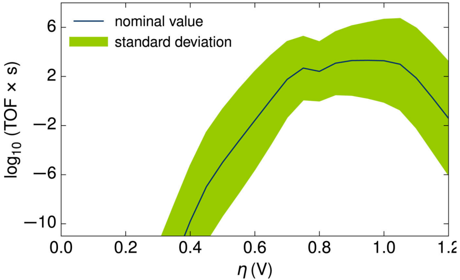

> *"Uncertainties depend strongly on reaction conditions and catalyst material, and the relative rates between different catalysts are considerably better described than the absolute rates."*

Medford *et al.*, Science, 2014, 345, 197.

Döpking *et al.*, J. Chem. Phys., 2018, 148, 034102.

Quantifying the impact of uncertainty on kinetic predictions

The correlated approach:
Assume DFT errors are correlated – introduce uncertainty in a scaled manner

Quantifying the impact of uncertainty on kinetic predictions

The correlated approach:
Assume DFT errors are correlated – introduce uncertainty in a scaled manner

1. Generate a normally distributed random number: $x \in N(0, 2\,\mathrm{kcal\,mol}^{-1})$

Quantifying the impact of uncertainty on kinetic predictions

The correlated approach:
Assume DFT errors are correlated – introduce uncertainty in a scaled manner

1. Generate a normally distributed random number: $x \in N(0, 2\,\mathrm{kcal\,mol^{-1}})$
2. Update relative free energies of all intermediates, I_j:

$$\Delta G_{I_j} = \Delta G_{I_j} + x$$

Quantifying the impact of uncertainty on kinetic predictions

The correlated approach:
Assume DFT errors are correlated – introduce uncertainty in a scaled manner

1. Generate a normally distributed random number: $x \in N(0, 2\,\mathrm{kcal\,mol^{-1}})$
2. Update relative free energies of all intermediates, I_j:

$$\Delta G_{I_j} = \Delta G_{I_j} + x$$

3. Generate uniformly distributed random numbers: $u_i \in U(0,1)\ \forall\ T_i$

Quantifying the impact of uncertainty on kinetic predictions

The correlated approach:
Assume DFT errors are correlated – introduce uncertainty in a scaled manner

1. Generate a normally distributed random number: $x \in N(0, 2\,\mathrm{kcal\,mol^{-1}})$
2. Update relative free energies of all intermediates, I_j:

$$\Delta G_{I_j} = \Delta G_{I_j} + x$$

3. Generate uniformly distributed random numbers: $u_i \in U(0, 1)\ \forall\ T_i$
4. Update relative free energies of all transition states, T_i:

$$\Delta G_{T_i} = \Delta G_{T_i} + xu_i$$

MK model more sensitive to perturbations than ES model

- **Large range** of predictions (boxes and whiskers)

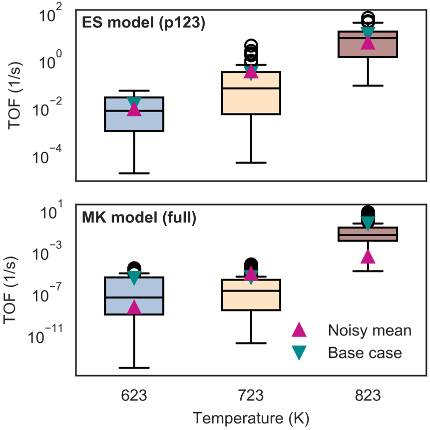

Energy span (most active path) vs microkinetic model predictions

Boje *et al.*, ChemRxiv, 2020.

MK model more sensitive to perturbations than ES model

- **Large range** of predictions (boxes and whiskers)
- Base case mostly **higher than median** (horizontal bars in the boxes)

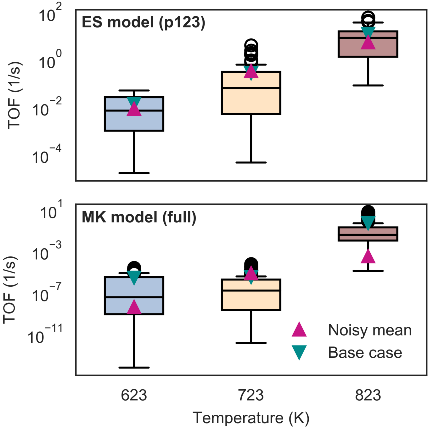

Energy span (most active path) vs microkinetic model predictions

Boje *et al.*, ChemRxiv, 2020.

MK model more sensitive to perturbations than ES model

- **Large range** of predictions (boxes and whiskers)
- Base case mostly **higher than median** (horizontal bars in the boxes)
- **Average** prediction generally **similar** (triangular markers)

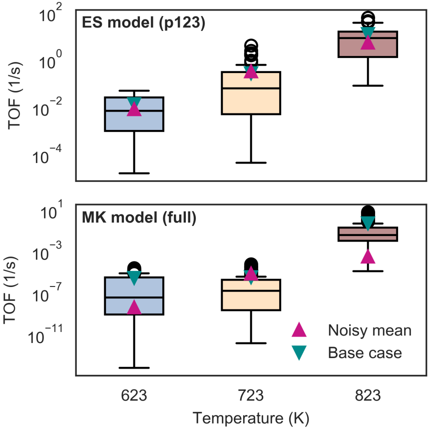

Energy span (most active path) vs microkinetic model predictions

Boje *et al.*, ChemRxiv, 2020.

MK model more sensitive to perturbations than ES model

- **Large range** of predictions (boxes and whiskers)
- Base case mostly **higher than median** (horizontal bars in the boxes)
- **Average** prediction generally **similar** (triangular markers)
- **Trends** with temperature **similar** (also for rate-determining states)

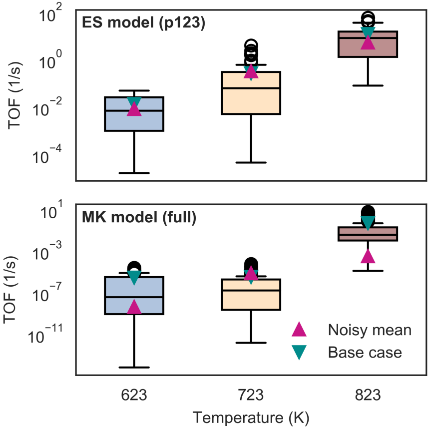

Energy span (most active path) vs microkinetic model predictions

Boje *et al.*, ChemRxiv, 2020.

Conclusions

Conclusions

1. **ES** and **MK** models informed by **DFT energies**

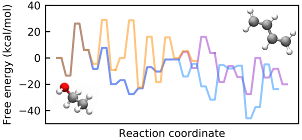

Conclusions

1. **ES** and **MK** models informed by **DFT energies**

2. **Dehydrogenation** more active than dehydration

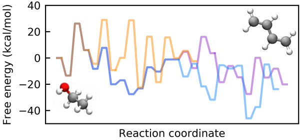

Conclusions

1. **ES** and **MK** models informed by **DFT energies**

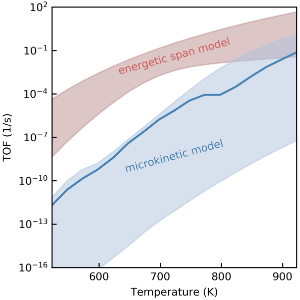

2. **Dehydrogenation** more active than dehydration

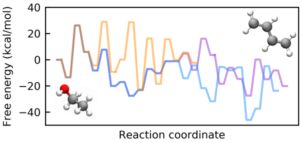

Conclusions

1. **ES** and **MK** models informed by **DFT energies**

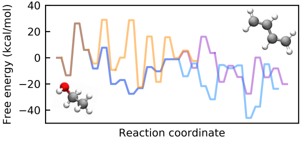

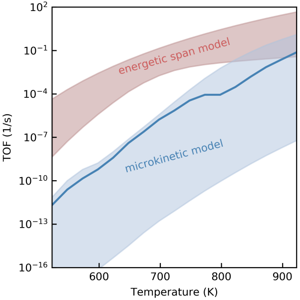

2. **Dehydrogenation** more active than dehydration

3. ES TOF $< 1\ s^{-1}$ at 723 K (MgO activity is low)

Conclusions

1. **ES** and **MK** models informed by **DFT energies**

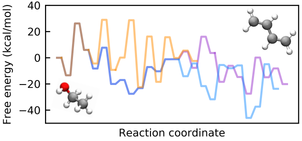

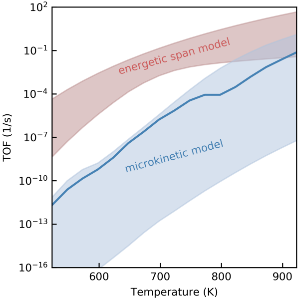

2. **Dehydrogenation** more active than dehydration

3. ES TOF $< 1\ s^{-1}$ at 723 K (MgO activity is low)

4. MK model has **lower turnover** and **higher uncertainty**

Conclusions

1. **ES** and **MK** models informed by **DFT energies**

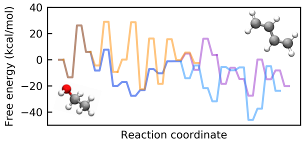

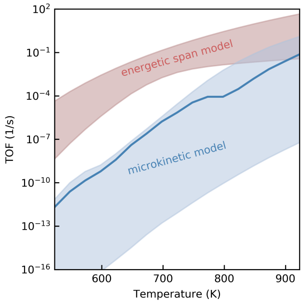

2. **Dehydrogenation** more active than dehydration

3. ES TOF $< 1\ s^{-1}$ at 723 K (MgO activity is low)

4. MK model has **lower turnover** and **higher uncertainty**

5. MK model accounts for **coverage, gas phase, competing pathways**

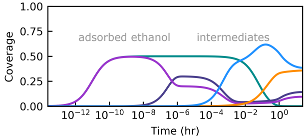

Conclusions

1. **ES** and **MK** models informed by **DFT energies**

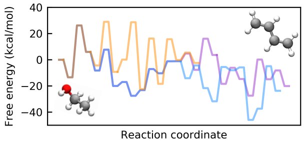

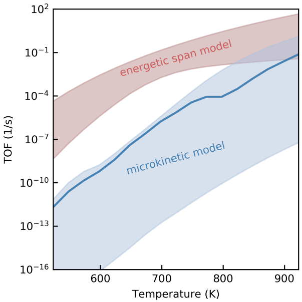

2. **Dehydrogenation** more active than dehydration

3. ES TOF $< 1\ s^{-1}$ at 723 K (MgO activity is low)

4. MK model has **lower turnover** and **higher uncertainty**

5. MK model accounts for **coverage, gas phase, competing pathways**

6. **High coverage** of ethanol, stable C_4 intermediates

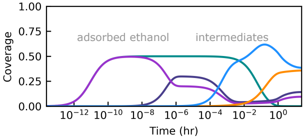

Acknowledgments

People:

Anders Hellman

Henrik Ström

Jonas Baltrusaitis

Tomáš Bučko

Funding:

Knut and Alice Wallenberg Foundation

Swedish Research Council

SNIC

NSC

NSF

XSEDE
Extreme Science and Engineering Discovery Environment

C3SE